Pre-print version of the paper published in Steel Construction 3/2017, DOI: 10.1002/stco.201710025

How placement of nut determines failure mode of bolt-and-nut assemblies

Erik L. Grimsmo*[,a], Arne Aalberg[b], Magnus Langseth[a], Arild H. Clausen[a]

[a]Structural Impact Laboratory (SIMLab) and Centre for Advanced Structural Analysis (CASA), Dept. Structural Engineering, Norwegian University of Science and Technology, Norway
[b] The University Centre in Svalbard, Norway
*Corresponding author. Email address: erik.l.grimsmo@ntnu.no.

Abstract

Bolt and nut assemblies under tension loading can either fail by bolt fracture or thread failure. The latter failure mode is arguably undesired because it leads to failure at a comparatively low deformation level. Moreover, incipient thread failure is challenging to detect in the case of over-tightening since the bolt remains in the bolt hole after this type of failure occurs. The failure mode of bolt and nut assemblies is determined by several well-known factors such as the thread engagement length and the relative strength of the bolt and nut. However, one factor that has received limited attention in the literature is the placement of the nut along the threaded portion of the bolt. We have performed a series of direct tension tests on various single M16 bolt and nut assemblies, where the placement of the nut was varied. Some of the assemblies experienced that placing the nut close to the thread run-out, i.e., near the unthreaded portion of the bolt (the shank), led to thread failure, whereas placing the nut sufficiently far from the thread run-out led to bolt fracture. We carried out finite element simulations of the tests in order to investigate further the mechanisms occurring during failure. In the case where the nut was located close to the thread run-out, the simulations revealed that necking of the bolt affected the effective overlap of the internal and external threads. This effect seemed to contribute to thread failure in both tests and simulations.

Keywords: bolts; experiments; simulations; thread failure

1 Introduction

It is common practice to use partially threaded bolts in connections subjected to shear forces such that the shear capacity of the unthreaded shank of the bolts may be utilized. Figure 1 illustrates a bolted end-plate connection imposed to a shear force V and a bending moment M, where using

partially threaded bolts can be beneficial for the resistance. The bending moment M induces tensile forces in the two upper rows of bolts, which implies that the tensile resistance and ductility of the bolt assemblies are of relevance as well. There are three failure modes of bolt assemblies under tension: bolt fracture, bolt thread failure, and nut thread failure. This paper demonstrates that employing partially threaded bolts in connections such as the one presented in Figure 1 can be unfavourable because thread failure more likely occurs than for connections with fully threaded bolts. Thread failure is a less ductile failure mode compared to bolt fracture, and may thus lead to premature failure of bolted joints. Furthermore, incipient thread failure may be challenging to detect during preloading of bolts because it is a gradual failure process. Consequently, a structure may enter service with partially failed bolts.

As an example, Grimsmo et al. [1] reported two replicate quasi-static tests on joints similar to the one in Figure 1, where the only difference between the two tests was that one test had two nuts per bolt instead of one. M16 bolts of grade 8.8 were used in the tests. The joint was designed so that failure occurred by a combination of end-plate bending and tensile bolt failure. The result in terms of moment-rotation of the joint is provided in Figure 2. As indicated in the figure, the test with one nut per bolt experienced thread failure, whereas the test with two nuts per bolt failed by bolt fracture. Clearly, the response of the test with two nuts per bolt is preferable, as both the bending moment resistance and the rotational capacity of the joint is increased. Thus, investigating the causes of thread failure is appropriate.

Several parameters, such as the relative strength between the bolt and nut, can determine the failure mode of bolt and nut assemblies under tension. However, the effect of the parameter denoted as threaded length L_t in Figure 3 seems to be unknown. To our knowledge, the technical paper by Alexander [2] is the only publication mentioning that this parameter can affect the failure mode of bolt assemblies. Alexander briefly describes how a short threaded length L_t may cause necking of

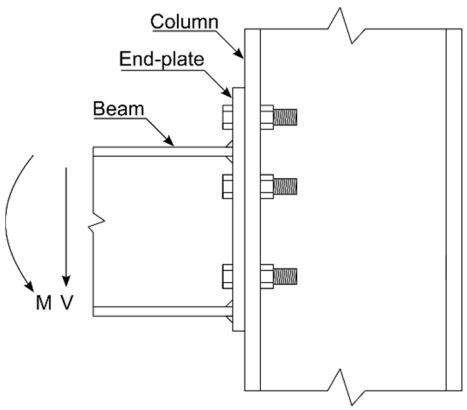

Figure 1 - Elevation view of a typical beam-to-column joint with end-plate connection.

the bolt to occur partly within the thread engagement length shown in Figure 3. Consequently, the overlap of the engaged threads of bolt and nut is affected, and thread failure becomes imminent. However, Alexander provided no experimental or numerical results. We therefore initiated an experimental program where we studied the effect of varying the threaded length L_t of bolt and nut assemblies subjected to direct tension loading. Additionally, finite element (FE) simulations of the tests were conducted to further investigate the mechanisms occurring during failure.

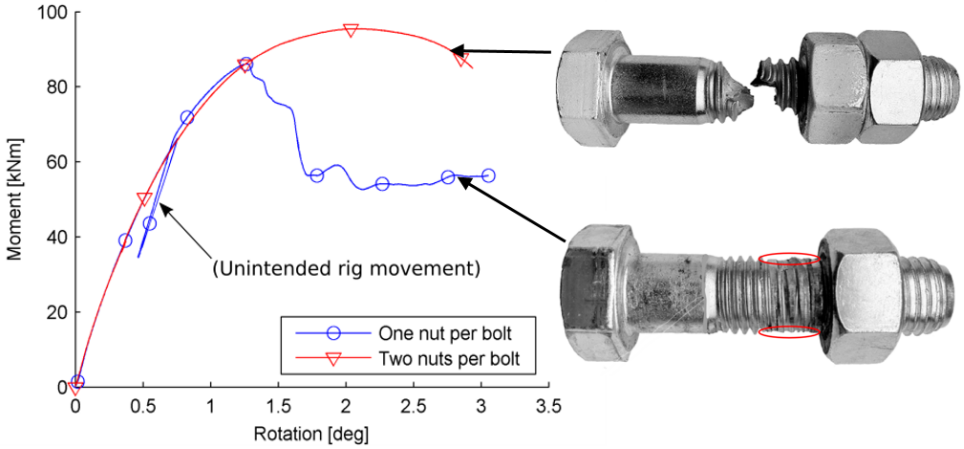

Figure 2 - Moment-rotation curves obtained from test on beam-to-column joints with bolted end-plate connections. One nut per bolt led to thread failure, whereas two nuts per bolt led to bolt fracture. See Grimsmo et al. [1] for more details.

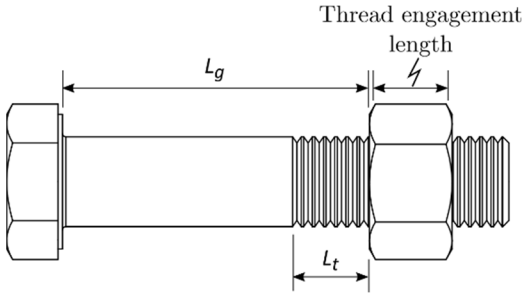

Figure 3 - Definitions of grip length L_g, threaded length L_t, and thread engagement length. Reprinted from Grimsmo et al. [3].

2 Experimental tests

2.1 Test specimens and setup

Figure 4a displays the various bolt and nut assemblies that were tested. Table 1 lists key information on the assemblies, such as the standards that specifies the geometry of the bolts and nuts. Note from the table that some of the bolts and nuts were marked with “SB” or “HR”. These markings indicate

that the bolt/nut was CE certified according to the standards EN 15048-1: *Non-preloaded structural bolting assemblies – Part 1: General requirements* [4] (SB) or EN 14399-3: *High-strength structural bolting assemblies for preloading – Part 3: System HR* [5] (HR). All the test specimens were M16 bolts and nuts with standard pitch, and they followed the property classes 8.8 and 8, respectively. The only exception was the nut of assembly number 5, which had property class 10.

A screw-driven tension/compression Instron machine with a capacity of 200 kN was employed for all the tests. The test specimens were mounted in the machine using two purpose-made grips, as shown in Figure 4b. Two circular steel plates of 20 mm thickness and with 18 mm bolt holes were placed in each grip. Thus, as the grips moved apart, the bolt and nut assembly was subjected to centric tension loading. The assemblies were loaded until failure with the displacement rates provided in Table 1. For assembly types 3-5, washers were used at both the bolt head and the nut. All assembly types were tested with different grip lengths L_g, and thus threaded lengths L_t; see Fig. 3 for definitions. Three to five replicate tests were conducted for each configuration of assembly and threaded length L_t, giving a total number of 95 tests. The applied force and cross-head displacement was logged in all tests. In addition, a digital camera monitored the specimens in some tests. The camera recordings were used to track the displacement of the head of the bolt and the nut using digital image correlation (DIC), hence the black-and-white pattern applied to the head and nut in Figure 4b. This allowed a local deformation measure that was convenient to compare with the subsequent FE simulation results. More details are provided by Grimsmo et al. [3], and Johansen and Waldeland [6].

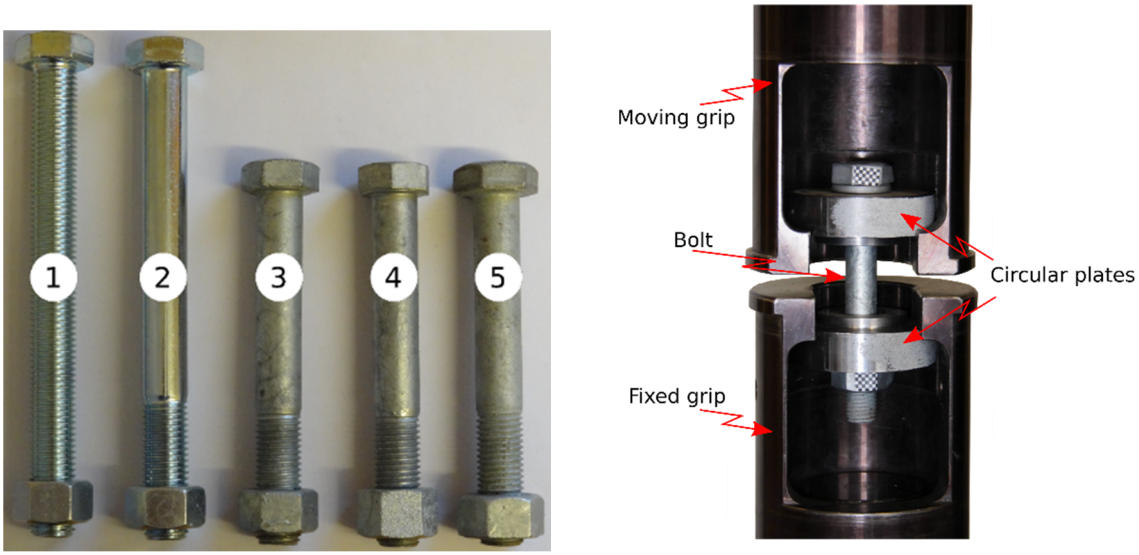

a) The five different bolt and nut assemblies b) A bolt and nut assembly mounted in the grips

Figure 4 - Photos of test specimens and test setup.

Table 1 - Key information on the tested bolt and nut assemblies. The numbering refers to Figure 4a. Abbreviations: SB=”structural bolts”, HR=”high resistance”, BZP=”bright zinc plating”, HDG=”hot dip galvanizing”.

No.	Bolt length [mm]	Bolt	Nut	Coating	Displ. rate [mm/min]	Failure mode
1	160	ISO 4017	ISO 4032	BZP	2.0	Bolt fracture
2	160	ISO 4014	ISO 4032	BZP	0.8	Bolt fracture or thread failure
3	120	ISO 4014 (SB)	ISO 4032 (SB)	HDG	0.6	Thread failure
4	120	ISO 4014 (SB)	ISO 4033	HDG	0.6	Bolt fracture
5	120	EN 14399 (HR)	EN 14399 (HR)	HDG	0.6	Bolt fracture or thread failure

2.2 Test results

As indicated in Table 1, the bolt and nut assemblies experienced either bolt fracture, thread failure, or both. A summary of the test results for each assembly type is provided here:

Type 1: This assembly type was the only one with fully threaded bolts. Bolt fracture occurred for all the tests. Necking of the bolt took place at a sufficient distance from the nut so that the overlap of the engaged threads was not affected.

Type 2: For this assembly type, a change in failure mode from bolt fracture to thread failure occurred as the threaded length L_t was reduced. Bolt fracture took place when $L_t \geq 17$ mm, i.e., eight or more full threads within the grip. Both failure modes were experienced for the intermediate range 11 mm $\leq L_t \leq$ 15 mm, whereas only thread

failure developed when $L_t \leq 9$ mm, which corresponds to having four full threads or less within the grip.

Type 3: Exclusively thread failure occurred for this assembly type (SB), which was tested for 5 mm $\leq L_t \leq$ 25 mm.

Type 4: This assembly type was tested with the same bolt type and range of threaded lengths L_t as assembly 3. The difference was that here we used a high nut (ISO 4033) instead of a regular nut (ISO 4032). Due to the longer thread engagement length obtained with a high nut, thread failure was avoided in all tests.

Type 5: Similar to what was observed for assembly 2, this assembly type (HR) experienced a transition of failure mode from bolt fracture to thread failure with decreasing threaded length L_t. Bolt fracture occurred when $L_t \geq 12$ mm, both failure modes were experienced when $L_t = 10$ mm, and thread failure took place when $L_t \leq 8$ mm.

As observed from these results, the threaded length L_t can clearly determine the failure mode for some bolt and nut assemblies. The results from assemblies 3 and 4 (regular vs. high nut) demonstrate that the thread engagement length also can affect the failure mode. Figure 5 displays force versus cross-head displacement of the test machine for four chosen threaded lengths L_t, acquired from tests on assembly type 2. Five replicate tests were carried out for each of these threaded lengths. Thread failure seemed to occur at maximum force, i.e., as necking of the bolt initiated. The necking occurred within the threaded portion of the bolt due to the reduced cross-sectional area of this region compared to the unthreaded bolt shank region. For short threaded lengths L_t, it appears that necking partly took place within the thread engagement length. This probably contributed to thread failure, and consequently a severe reduction in the cross-head displacement at failure, as shown in Figure 5. The simulation results in Section 3 demonstrate that necking of the bolt indeed contributes to thread failure.

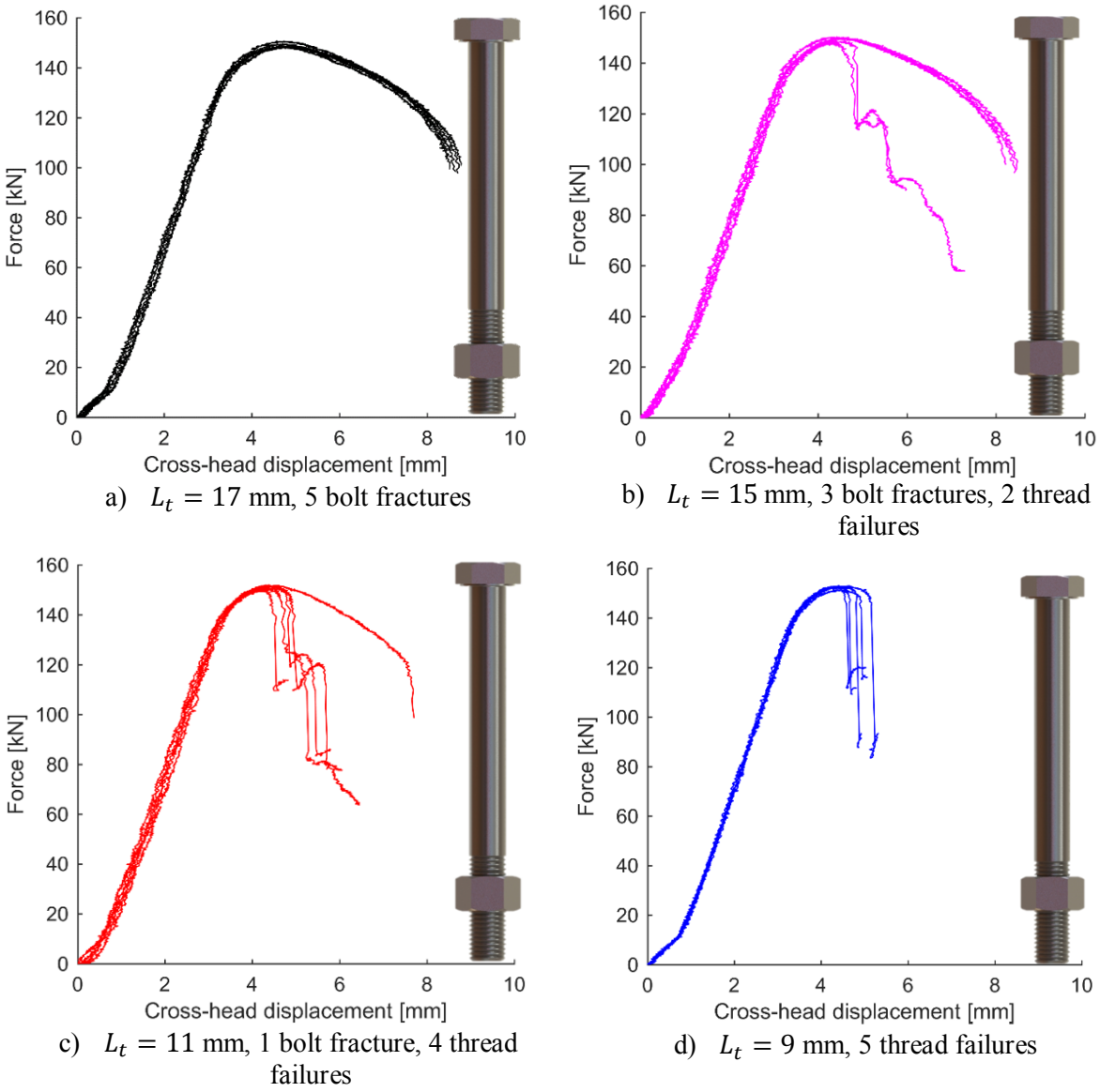

a) $L_t = 17$ mm, 5 bolt fractures

b) $L_t = 15$ mm, 3 bolt fractures, 2 thread failures

c) $L_t = 11$ mm, 1 bolt fracture, 4 thread failures

d) $L_t = 9$ mm, 5 thread failures

Figure 5 - Force-displacement curves obtained from tests on assembly type 2 (see Table 1). Five replicate tests were performed for each threaded length L_t.The figure of the bolt and nut assembly on the right hand side of the plots indicates the position of the nut for the respective tests.

3 Numerical simulations

3.1 Geometry, mesh, and boundary conditions

The FE model and simulations presented in this paper are based on the tests on assembly type 2, i.e., the assembly with 160 mm long partially threaded bolt and no SB/HR marking. The simulations were carried out with Abaqus/Explicit v6.14. An axisymmetric model of the tests was developed; see Figure 6. Obviously, an axisymmetric model cannot capture the helical shape of the threads, and some simplifications with regard to the geometry was therefore be made. However, for the purposes of this study, the model produced sufficiently accurate results (see Johansen and

Waldeland [6] for comparison of simulations with an axisymmetrical model and a 3D model with helical threads).

As illustrated in Figure 6a, the bottom circular plate was fixed, whereas the top circular plate was subjected to a displacement rate of 0.8 mm/s. Thus, load conditions similar to those in the tests were achieved. Surface-to-surface contact interactions were established between appropriate surfaces, and a friction coefficient of 0.2 was assumed. Figure 6b displays the element mesh of the thread engagement region. The approximate element sizes were 0.1 mm in the threads, 0.4 mm in the remaining part of the nut and threaded portion of the bolt, and 1.0 elsewhere. Quadrilateral axisymmetric elements with reduced integration were employed. The total number of elements was approximately 9000. Mass scaling was used to reduce the computational time. For more details, see Grimsmo et al. [3].

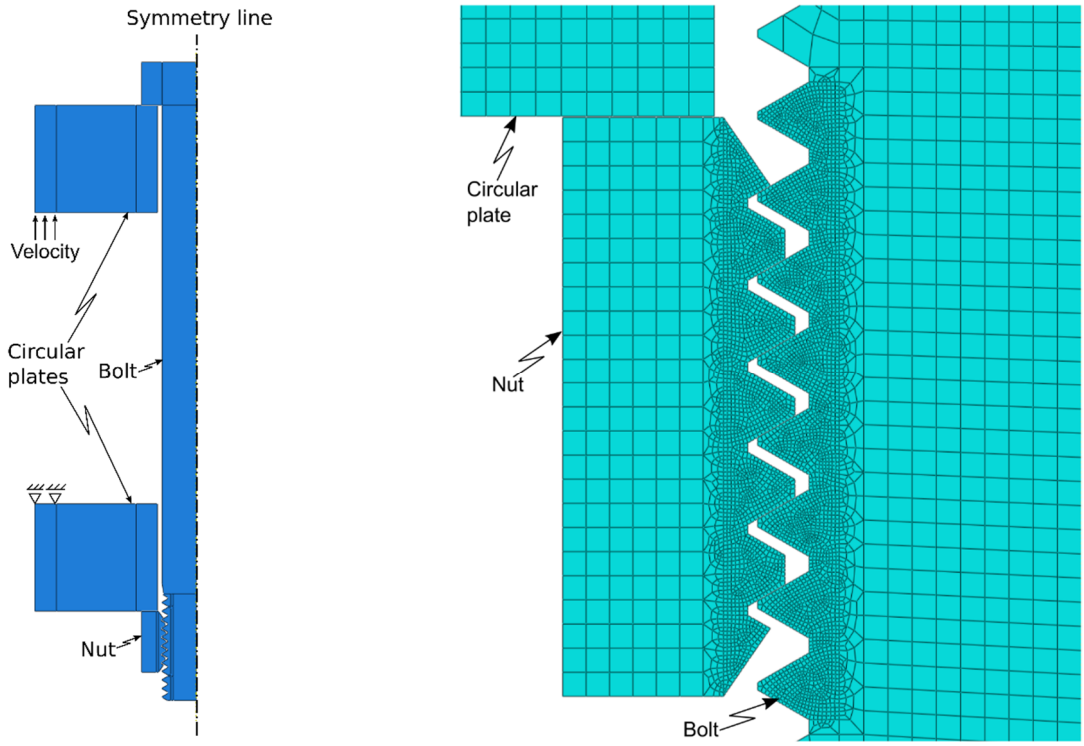

a) Elevation view of entire model b) Mesh of thread engagement region

Figure 6 - The axisymmetric FE model of the tests. Reprinted from Grimsmo et al. [3].

3.2 Material modelling

An elastic-viscoplastic constitutive relation was chosen for the material of the bolt and nut. The relation comprised linear isotropic elasticity, the von Mises yield criterion, an associated flow rule,

non-linear isotropic hardening, and strain-rate hardening. A Young's modulus of 210 GPa and Poisson's ratio of 0.3 were assumed. The equivalent stress σ_{eq} was given by

$$\sigma_{eq} = \begin{cases} \sigma_y, & \varepsilon_p < \varepsilon_{p,plat} \\ \left[\sigma_y + \sum_{i=1}^{2} Q_i \left(1 - \exp\left(-\frac{\theta_i}{Q_i}\left(\varepsilon_p - \varepsilon_{p,plat}\right)\right)\right)\right]\left[1 + \frac{\dot{\varepsilon}_p}{\dot{\varepsilon}_{ref}}\right]^C, & \varepsilon_p \geq \varepsilon_{p,plat} \end{cases} \quad (1)$$

where σ_y is the yield stress; Q_i and θ_i (where $i = \{1,2\}$) are the hardening constants of the extended Voce hardening rule; ε_p is the equivalent plastic strain; $\varepsilon_{p,plat}$ is the value of ε_p at the end of the yield plateau; $\dot{\varepsilon}_{ref}$ is the reference strain rate; and C is a constant. Obviously, the second square brackets of Equation 1 governs the strain-rate sensitivity of the material. Viscous effects were included because a significant increase of the strain rate was observed in the deforming threads during failure.

The extended Cockcroft-Latham failure criterion proposed by Gruben et al. [7] was implemented in the material model. The damage D at the integration points of the elements was described by

$$D = \frac{1}{W_c} \int_0^{\varepsilon_p} \left\langle \phi \frac{\sigma_I}{\sigma_{eq}} + (1 - \phi) \frac{(\sigma_I - \sigma_{III})}{\sigma_{eq}} \right\rangle^{\gamma} \sigma_{eq} \mathrm{d}\varepsilon_p \quad (2)$$

where the fracture parameters W_c, ϕ, and γ are constants; $\langle \cdot \rangle$ are the Macaulay brackets ensuring nonnegative integrand; σ_I and σ_{III} are the first and third principal stress of the Cauchy stress tensor. $D = 0$ indicates zero damage in the material, whereas $D = 1$ means failure of the material at the integration point. Thus, as the integral in Equation 2 reached the critical value W_c at the integration point, the parent element was deleted (elements with one integration point were employed).

The procedure for identifying the material parameters involved uniaxial tension tests of the bolt material and inverse FE modelling of these tests. The procedure is described in detail by Grimsmo et al. [3]. The values of the parameters used for the bolt material are listed in Table 2. Note that the values for $\dot{\varepsilon}_{ref}$ and C are were adopted from Grimsmo et al. [8], and ϕ and γ were adopted from Gruben et al. [9]. The material parameters used for the bolt was also employed for the nut, except that the yield stress σ_y for the nut was set to 697.4 MPa, which was derived from hardness tests performed on the bolt and nut material [3].

Table 2 - Parameters used for the bolt material in the FE simulations.

σ_y [MPa]	Q_1 [MPa]	θ_1 [MPa]	Q_2 [MPa]	θ_2 [MPa]	$\varepsilon_{p,plat}$ [-]	$\dot{\varepsilon}_{ref}$ [1/s]	C [-]	W_{cr} [MPa]	ϕ [-]	γ [-]
908.7	99.70	5194	3131	293.6	0.013	0.001	0.011	1480	0.355	1.550

3.3 Simulation results

Here we present results from simulations where the threaded length L_t was 9 and 17 mm. Recall from Section 2.2 and Figure 5 that the corresponding tests experienced exclusively thread failure and bolt fracture, respectively. Figure 7 shows results obtained with $L_t = 17$ mm. As for the corresponding tests, bolt fracture occurred in the simulation. Considering the force-displacement curves in Figure 7b, a good agreement between tests and simulation is observed, particularly up to approximately 5 mm displacement. The abscissa in this figure is the relative displacement between the bolt head and the nut. At 5 mm displacement, the curves deviate somewhat from each other, and an 18% larger displacement at failure was obtained in the simulation. A possible explanation for this increased failure displacement is related to the axisymmetry of the model. As can be observed from Figure 7a, one thread is located approximately at the centre of the neck. Thus, the effective diameter of the bolt at this location is given by the major diameter of bolt threads. This gives an unrealistically large diameter at the centre of the neck because a helical shape of the threads would give an effective diameter that is the average of the major and minor diameter of the bolt threads.

a) Failure by bolt fracture occurred in the simulation

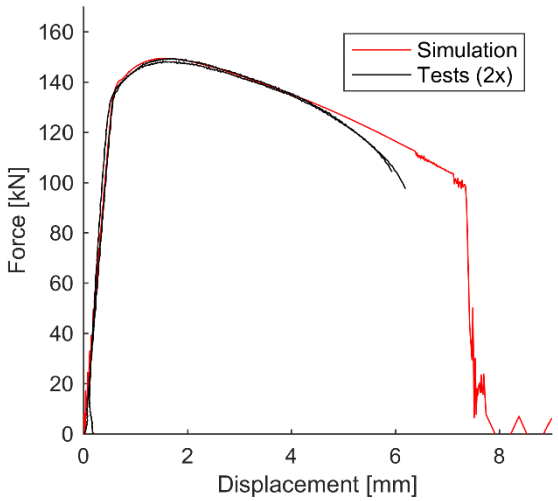

b) Force-displacement curves obtained from two replicate tests and the corresponding simulation

Figure 7 - Results with $L_t = 17$ mm. Bolt fracture occurred in the tests and simulation. Reprinted from Grimsmo et al. [3].

Figure 8 displays the evolution of deformation of initially engaged threads obtained from a simulation with the shorter threaded length $L_t = 9$ mm. Thread failure clearly occurred in the simulation, as was experienced for the five corresponding tests. Although difficult to discern from

Figure 8, the bolt contracted radially throughout the simulation. This contraction occured due to elongation and necking of the bolt. Obviously, necking did not occur before maximum load was reached. The consquence of the contraction was that pair ① of initially engaged threads disengaged, as seen in the bottom frame of Figure 8. Consequently, the remaining engaged threads had to carry the load, which eventually led to thread failure. Note that this disengaging of threads did not occur with L_t = 17 mm (see Figure 7a). Figure 8 display that pair ② of engaged threads experienced significant shear deformation and fracture, visible by element deletion. For pair ③ of engaged threads, a combination of shear and bending deformation occurred, but no fracture was observed for the applied displacement.

Figure 9 depicts the force-displacement curves of the simulation with $L_t = 9$ mm and two corresponding tests. Again, a good agreement is observed between the simulation and the tests. For this case, also the displacement at failure is well captured by the simulation. Note that the minor oscillations in the start and end of the simulation curve is due to the mass scaling, but they have practically no impact on the global response.

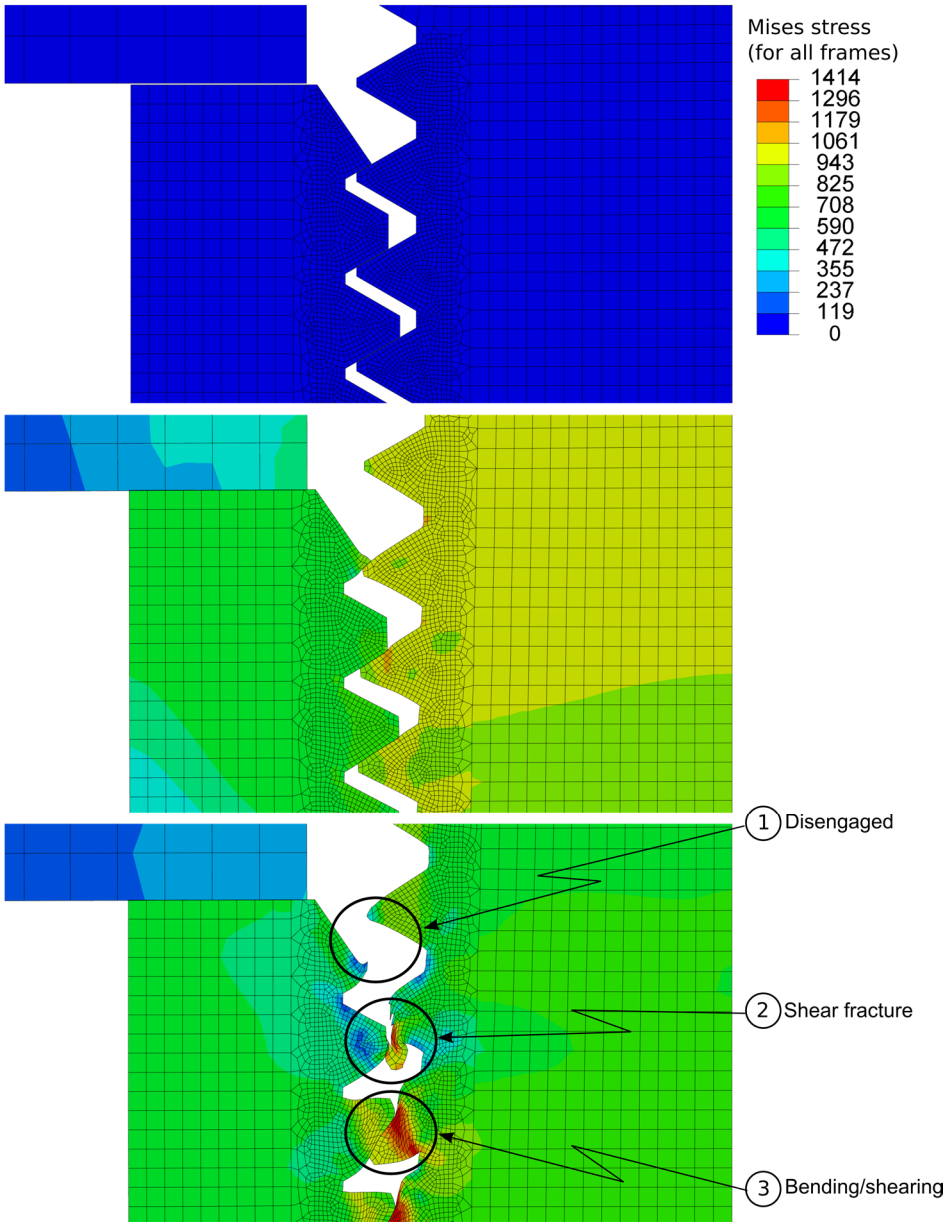

Figure 8 - Deformed threads at three stages throughout a simulation with $L_t = 9$ mm. The numbers 1 to 3 in the bottom frame label the pairs of engaged threads. Reprinted from Grimsmo et al. [3].

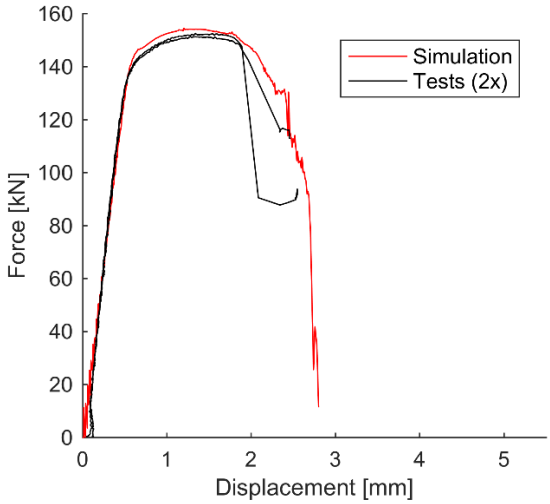

Figure 9 - Force-displacement curves obtained from two replicate tests with $L_t = 9$ mm and the corresponding simulation. Reprinted from Grimsmo et al. [3].

4 Discussion

As mentioned, assembly type 5 complies with the requirements of the HR system. Assemblies that conform to this system are designed so that deformation should predominantly occur by plastic elongation of the bolt [5]. It is therefore interesting that this assembly type experienced thread failure for threaded lengths $L_t \leq 10$ mm, which corresponds to having five full threads within the grip. The code EN 1090-2: *Execution of steel structures and aluminium structures – Part 2* [10] states that non-preloaded assemblies require at least one full thread (in addition to the thread run-out) in the grip, and four full threads in the grip for preloaded assemblies. Note that the purpose of these requirements is to prevent jamming of the nut on the thread run-out section, and not to inhibit thread failure. It should also be mentioned that the standard for SB assemblies does not specify any intended failure mode.

It can be argued that thread failure is preferred over bolt fracture in some cases because bolt and nut assemblies that have failed by thread failure due to over-tightening during preloading still functions as non-preloaded assemblies. This is the philosophy of the assemblies following the HV system, i.e., EN 14399-4: *High-strength structural bolting assemblies for preloading - Part 4: System HV* [11]. These assemblies have lower nuts, which leads to shorter thread engagement lengths than with regular nuts. Thus, plastic deformation predominantly occurs by thread deformation for HV assemblies. Since thread failure takes place at a comparatively low deformation level, these assemblies are relatively sensitive to over-tightening, and hence require more on-site inspections than assemblies that are designed for bolt fracture. This aspect together

with possibly reducing the resistance and deformation capacity of bolted joints (ref. Figure 2) makes thread failure generally undesired.

The tests and simulations presented in this paper demonstrate that increasing the threaded length L_t can reduce the probability of thread failure. Increasing this length for standard partially threaded bolts can be achieved by employing washers and shims. Another approach is rather to use fully threaded bolts. This approach is possibly more appealing because using fully threaded bolts also simplify stock holding and improve construction efficiency since the number of different bolts can be reduced, as argued by Owens [12].

5 Summary

Various types of M16 bolt and nut assemblies were subjected to direct tension loading. The threaded length L_t (i.e., the distance from the nut to the thread run-out) was varied among the tests, and three to five replicate tests were conducted for each configuration. For two of the five tested assembly types, a transition from bolt fracture to thread failure was experienced as the threaded length L_t was reduced. Thus, L_t can clearly affect the failure mode of bolt and nut assemblies. Also in the FE simulations of the tests did L_t determine the failure mode, and a similar behaviour as in the tests was obtained, both in terms of global response and local failure mechanisms. Furthermore, the simulations revealed that if L_t was sufficiently small, necking of the bolt reduced the overlap of the engaged threads, which contributed to thread failure.

Acknowledgements

The work has received financial support from the Research Council of Norway through the SFI scheme. We would like to thank MSc. E. Skavhaug and MSc. S. Østhust for the help with testing assembly types 1 and 2, and MSc. S. Johansen and MSc. E. Waldeland for carrying out the tests on assembly types 3-5. We would also like express our gratitude towards Prof. Emeritus P. K. Larsen for feedback on the work.

References

[1] E.L. Grimsmo, A.H. Clausen, M. Langseth, A. Aalberg, An experimental study of static and dynamic behaviour of bolted end-plate joints of steel, Int J Impact Eng, 85 (2015) 132-145.

[2] E.M. Alexander, Analysis and design of threaded assemblies, in: SAE Transactions, 1977.

[3] E.L. Grimsmo, A. Aalberg, M. Langseth, A.H. Clausen, Failure modes of bolt and nut assemblies under tensile loading, J Constr Steel Res, 126 (2016) 15-25.
[4] European Committee for Standardization (CEN), NS-EN 15048-1, Non-preloaded structural bolting assemblies - Part 1: General requirements, Norwegian Standard, 2007.
[5] European Committee for Standardization (CEN), NS-EN 14399-3, High-strength structural bolting assemblies for preloading - Part 3: System HR - Hexagon bolt and nut assemblies, Norwegian Standard, 2015.
[6] S. Johansen, E. Waldeland, An experimental and numerical study of bolt and nut assemblies under tension loading (master thesis), in, Norwegian University of Science and Technology, 2016.
[7] G. Gruben, O.S. Hopperstad, T. Borvik, Evaluation of uncoupled ductile fracture criteria for the dual-phase steel Docol 600DL, Int J Mech Sci, 62 (2012) 133-146.
[8] E.L. Grimsmo, A.H. Clausen, A. Aalberg, M. Langseth, A numerical study of beam-to-column joints subjected to impact, Eng Struct, 120 (2016) 103-115.
[9] G. Gruben, O.S. Hopperstad, T. Børvik, Simulation of ductile crack propagation in dual-phase steel, Int J Fracture, 180 (2013) 1-22.
[10] European Committee for Standardization (CEN), NS-EN 1090-2: Execution of steel structures and aluminium structures - Part 2: Technical requirements for steel structures, Norwegian Standard, 2008.
[11] European Committee for Standardization (CEN), NS-EN 14399-4, High-strength structural bolting assemblies for preloading - Part 4: System HV - Hexagon bolt and nut assemblies Norwegian Standard, 2015.
[12] G.W. Owens, The use of fully threaded bolts for connections in structural steelwork for buildings, The Structural Engineer, 70 (1992) 297-300.